Available online at www.sciencedirect.com
ScienceDirect
Catalysis Today 132 (2008) 138–145
CATALYSIS TODAY
www.elsevier.com/locate/cattod

Effect of $NaBH_4$ concentration on the characteristics of PtRu/C catalyst for the anode of DMFC prepared by the impregnation method

Min-Soo Hyun [a,b], Sang-Kyung Kim [a,*], Byungrock Lee [a], Donghyun Peck [a], Yonggun Shul [b], Doohwan Jung [a]

[a] *Advanced Fuel Cell Research Center, Korea Institute of Energy Research, 71-2 Jang-dong, Yuseong-gu, Daejeon 305-343, Republic of Korea*
[b] *Department of Chemical Engineering, Yonsei University, Seoul 120-749, Republic of Korea*

Available online 24 January 2008

Abstract

PtRu/C catalysts were prepared using an aqueous co-impregnation method with $NaBH_4$ as a reducing agent. In order to investigate the effect of the reducing agent concentration, metal ions were reduced in different $NaBH_4$ concentrations for which the molar ratios of $NaBH_4$ to metal ions were controlled to 1, 2, 5, 15, 50, and 250. The electrochemical properties were studied by cyclic voltammetry in a 0.5 M H_2SO_4 solution. The surface compositions and oxidation states of the catalysts were observed by X-ray photoelectron spectroscopy (XPS). According to the X-ray diffraction (XRD) results, Pt (fcc) peak shifts were observed and crystal sizes were calculated. The electro-catalytic activities of the prepared catalysts for methanol electro-oxidation were estimated using linear sweep voltammetry. Unit cell tests were carried out to compare the direct methanol fuel cell performances. The $NaBH_4$ concentration was found to affect the dispersion and the surface composition of the prepared PtRu particles. Optimum molar ratios of $NaBH_4$ to metal ions were 5 and 15 for methanol electro-oxidation.

Keywords: PtRu catalyst; Impregnation; Direct methanol fuel cell

1. Introduction

PtRu alloy is generally regarded as the most appropriate catalyst for methanol electro-oxidation. It is known that Ru easily removes CO from Pt atoms and enhances the catalytic activity of methanol electro-oxidation by a bifunctional mechanism or a ligand effect [1–3]. However, the possibility of the commercialization of direct methanol fuel cell (DMFC) remains unclear due to the low power density caused by the low catalytic activity for methanol oxidation and due to methanol crossover through the membrane. Many researchers have sought to improve the activity of the PtRu catalyst in various approaches. One such technique increases the active surface area using the carbon support, which has a large surface area and high electron conductivity. Carbon black has being used as a catalyst support of commercial products. Nano-structured carbon materials such as carbon nanotubes [4,5], carbon nanofibers [6,7] or mesoporous carbon [8,9] made using a template method have recently been studied as new catalyst supports. Another approach is to add one or more elements into the PtRu alloy to make ternary or quaternary catalysts [10–15]. A third is to make the catalyst particles smaller and more dispersive on the carbon support, which is possible through a variety of techniques.

It is fundamentally important to make metal ions to metal seeds and then to grow the metal seeds uniformly into small particles because a highly dispersed catalyst particle is essential for a large active surface area. There are several methods to synthesize PtRu nano-particles for fuel cell application including the impregnation method, the colloidal method, the micro-emulsion method, and the polyol method [16–22]. Among these methods, the impregnation method is most widely used because the process is simple. This method includes many variables, such as the use of different reducing

* Corresponding author. Tel.: +82 42 860 3366; fax: +82 42 860 3309.
E-mail address: ksk@kier.re.kr (S.-K. Kim).

0920-5861/$ – see front matter
doi:10.1016/j.cattod.2007.12.034

agent and metal precursors, as well as different means of mixing the reducing agent and changing the pH, which affects the particle size, dispersion, morphology, surface composition, and degree of alloying.

In this work, the effect of the $NaBH_4$ concentration as the reducing agent is investigated via an aqueous co-impregnation method. PtRu/C catalysts were prepared via an impregnation method under different $NaBH_4$ concentrations. Each sample

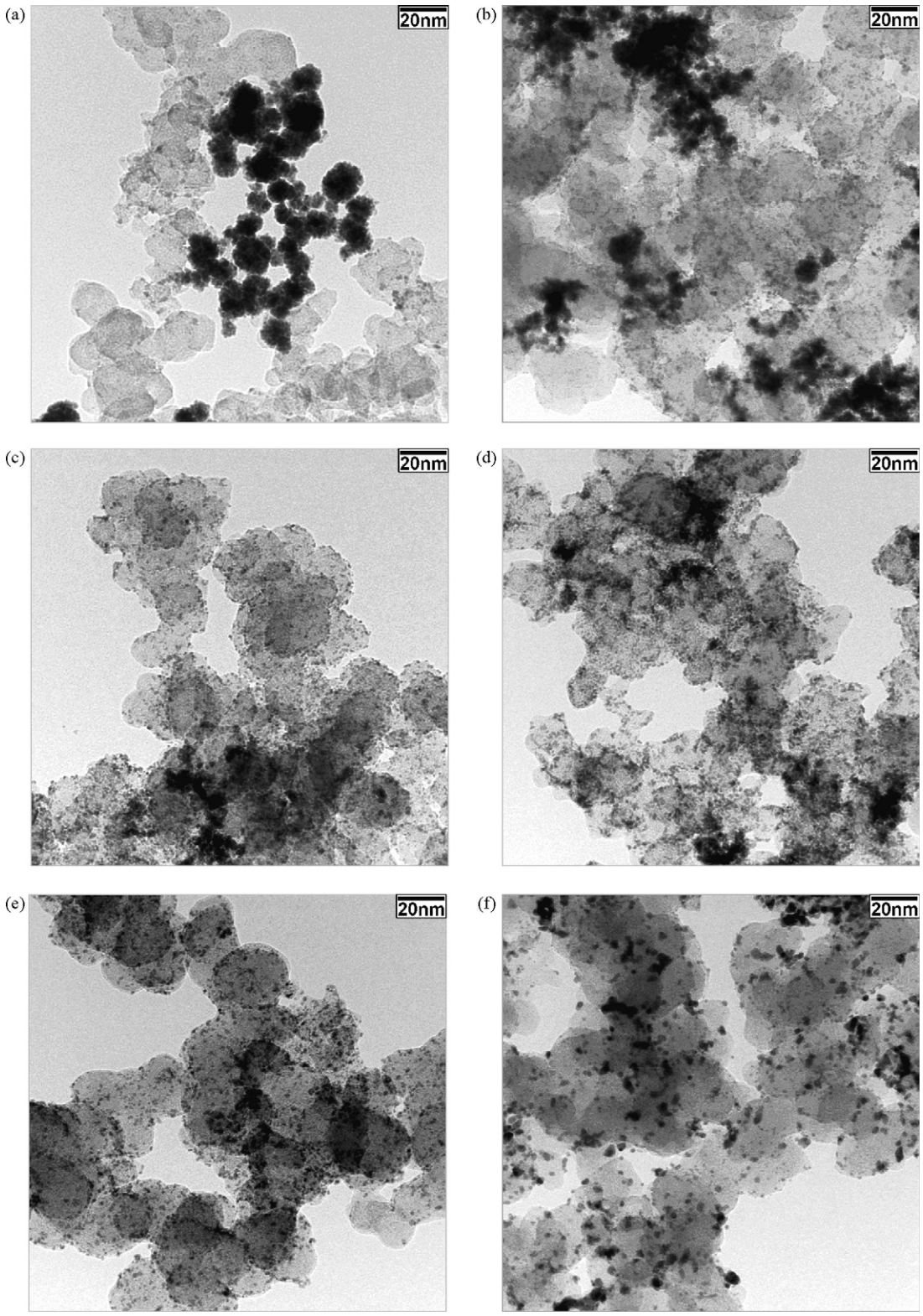

Fig. 1. TEM images of the prepared catalysts: (a) x1, (b) x2, (c) x5, (d) x15, (e) x50 and (f) x250.

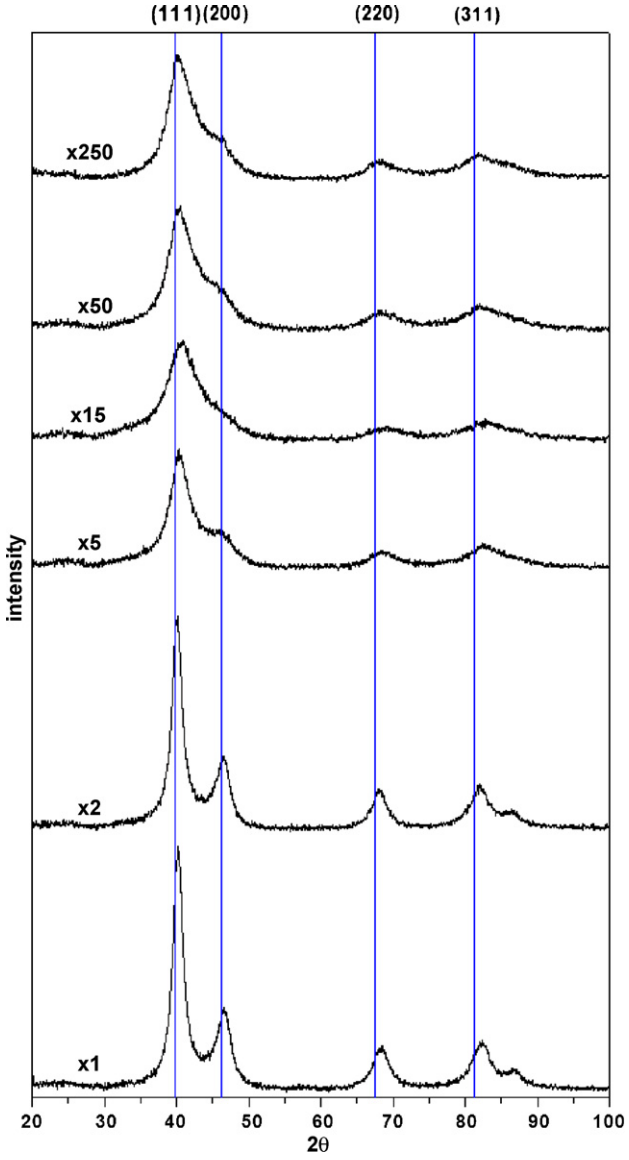

Fig. 2. X-ray diffraction patterns of the prepared catalysts.

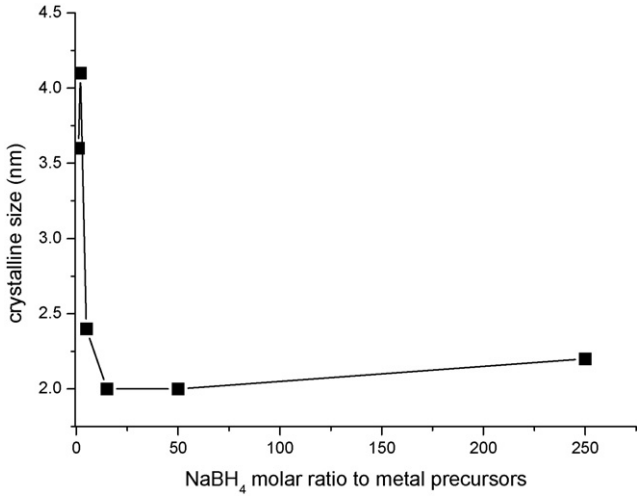

Fig. 3. Crystal size change with the molar ratio of $NaBH_4$ to metal precursor.

was then analyzed by transmission electron microscopy (TEM), cyclic voltammetry (CV), X-ray photoelectron spectroscopy (XPS) and X-ray diffraction (XRD). Unit cell performances were also tested for use with direct methanol fuel cells with the prepared catalysts.

2. Experimental

2.1. Preparation of PtRu/C catalysts

Carbon black, Vulcan-P (about 150 $m^2\ g^{-1}$ BET surface area) from the Cabot Corporation was suspended in deionized water and sonicated. H_2PtCl_6 and $RuCl_3$ were dissolved in deionized water and stirred. These two solutions were mixed together and stirred sufficiently. The amounts of metal precursors were adjusted that Pt and Ru had a molar ratio of 1:1 and the total metal content in the catalyst was 60 wt%. $NaBH_4$ solutions of different concentrations were prepared in which the molar ratio of $NaBH_4$ to Pt and Ru metals was 1, 2, 5, 15, 50 and 250. The mixed solutions of the carbon black and metal ions were poured into each $NaBH_4$ solution rapidly. After 20 min the prepared catalysts were filtered and washed with boiling water for 3 h. The catalysts were then dried in vacuum oven at 80 °C for 12 h. The catalysts prepared using 1, 2, 5, 15, 50 and 250 times of the $NaBH_4$ molar content to the metal precursors were designated as 'x1', 'x2', 'x5', 'x15', 'x50' and 'x250', respectively.

2.2. Characteristics of PtRu/C catalysts

Transmission electron microscopy (TEM) images of the prepared catalysts were obtained by a Philips TECNAI F20, and powder X-ray diffraction (XRD) patterns were recorded on a

Table 1
Properties of the crystal and surface of the prepared catalyst from XRD and XPS results

Catalyst name	Position of fcc (1 1 1) (2θ)	Lattice constant (Å)	Crystal size (nm)	Oxidation state of Pt relative amount (%)		Surface composition Pt:Ru (%)
				Pt^0	Pt^{2+} or Pt^{4+}	
x1	40.20	3.88	3.6	48.3	51.7	12:88
x2	40.10	3.89	4.1	53.1	46.9	25:75
x5	40.32	3.863	2.4	42.3	57.7	52:48
x15	40.70	3.83	2.0	37.9	62.1	59:41
x50	40.27	3.874	2.0	48.1	51.9	59:41
x250	40.18	3.883	2.2	53.0	47.0	63:37
Commercial PtRu/C	–	–	–	36.7	63.3	46:54

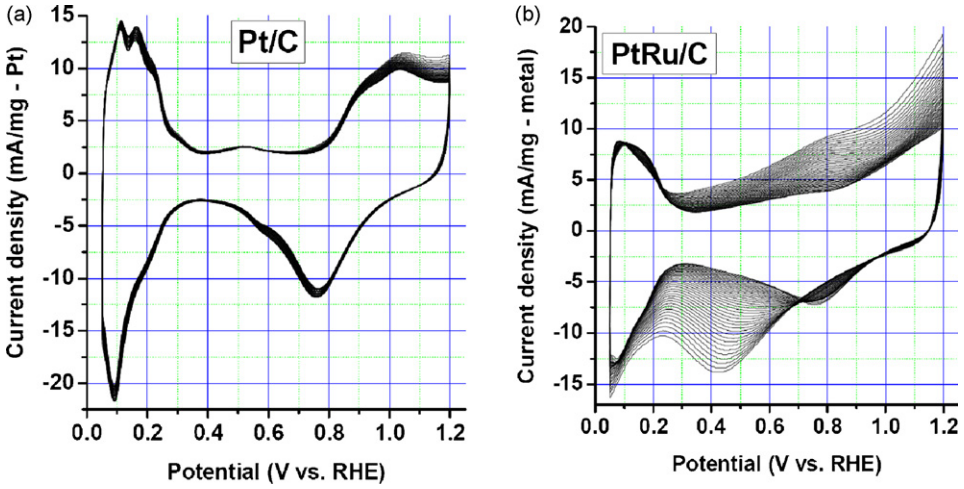

Fig. 4. Cyclic voltammograms of the commercial catalysts in 0.5 M H_2SO_4 solution at the scan rate of 20 mV/s: (a) commercial Pt/C and (b) commercial PtRu/C.

Rigaku D/MAX-IIIC X-ray diffractometer using Cu Kα radiation. The crystal sizes were calculated from the XRD results using the Debye–Scherrer equation. X-ray photoelectron spectroscopy (XPS) were analyzed with an ESCA-LAB MK II from VG Scientific LTD using Mg Kα radiation, and the binding energies were calibrated with a C 1s value of 284.6 eV.

2.3. Electrochemical measurements

For the cyclic voltammetry and the linear sweep voltammetry, a platinum mesh and an Ag/AgCl electrode were used as the counter electrode and the reference electrode, respectively. To make a working electrode catalyst inks were prepared by dispersing the catalyst powder in ethanol and Nafion solutions. Ten microliters of the catalyst ink was dropped on a glassy carbon electrode and dried. In all cases, it was adjusted that 0.158 mg of the catalyst was loaded and the Nafion polymer content of the catalyst layer was 5 wt%. The temperature of the half-cell equipment was maintained at 25 °C and dissolved oxygen was removed by bubbling nitrogen through the solution.

Membrane electrode assemblies (MEAs) were prepared by hot pressing Nafion 115 and catalyst-coated electrodes to measure the performance of a direct methanol fuel cell. HiSPEC 1000 Pt black from Johnson Matthey was used as a cathode catalyst with Pt loading of 5 mg/cm^2. Pt loading of the prepared catalysts for the anode was 2 mg/cm^2.

3. Results and discussion

Transmission electron microscopy (TEM) images of the prepared catalysts are presented in Fig. 1. The 10–30 nm spherical particles are carbon blacks and the dark dots that measure approximately 2 nm are the PtRu metal alloys supported on the carbon blacks. The precursors designated x1 and x2 are less dispersive and x250 has larger metal particles compared to the other catalysts.

X-ray diffraction (XRD) patterns are shown in Fig. 2. For pure Pt crystal, the peaks at 39.763°, 46.243°, 67.454° and 81.286° are assigned to the (1 1 1), (2 0 0), (2 2 0) and (3 1 1) planes, respectively, of a face-centered cubic (fcc) structure [23]. The XRD patterns of the prepared catalysts were slightly shifted to higher angles from the Pt. This shows that Pt formed a solid solution with Ru by replacing Pt atoms with Ru atoms in the fcc structure of the Pt crystal [24,25]. The peak position of fcc (1 1 1), the lattice constant and the crystal size derived from the XRD results are presented in Table 1. Crystal size was obtained from the peak of fcc (2 2 0) using the Debye–Scherrer equation. In the XRD patterns of the prepared catalysts, a difference in the intensities in the (2 0 0) peak was observed. x15 showed a small (2 0 0) peak while x1 and x2 showed stronger (2 0 0) peaks. Kim et al. [25] found that the intensities of fcc (2 0 0) peak decreased with the increase of Ru content from 30% to 60% by examining the grazing incidence X-ray diffraction (GIXD). Therefore, it can be predicted that x15 includes a higher amount of Ru in the PtRu solid solution compared to either x1 or x2. In addition, the small lattice constant of x15 implies that x15 has the highest degree of alloying of solid solution. Fig. 3 shows the effect of the reducing agent concentration on the crystal size. It was observed that the crystal size increased below x5. The effect of the reducing agent concentration on the particle size of PtRu catalyst was investigated in earlier studies [21,22]. Large particles are generally created under low concentrations of reducing agent as the nuclei growth is faster than the nucleation.

Fig. 4 shows the cyclic voltammograms of commercial Pt/C and PtRu/C for 40 cycles. PtRu/C showed three different characteristics compared with Pt/C. First, the base current around 0.4 V decreased with the number of cycles and the base current in the backward scan was larger than that of the forward scan. The base current of the backward scan changed from −10 mA/mg to −3 mA/mg. This high base current originated from the pseudo-capacitance, which generally increases with the Ru content [26,27]. Gojkovic et al. [26] confirmed that the pseudo-capacitance increases with increase in the Ru content in the PtRu catalyst due to adsorbed OH-groups on the Ru. Second, the hydrogen desorption peak from 0.05 V to 0.3 V increased as the cycles repeated. The hydrogen desorption

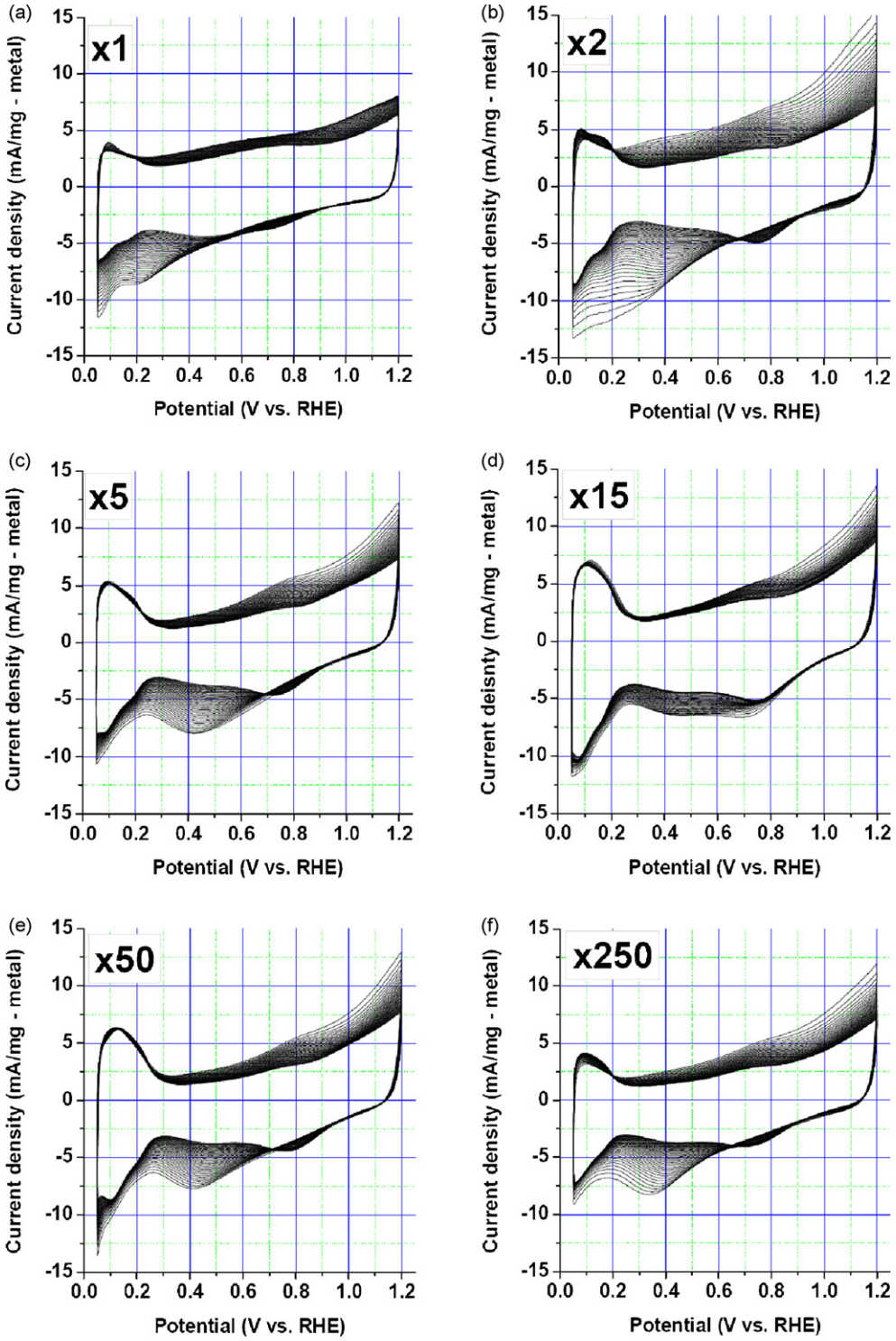

Fig. 5. Cyclic voltammograms of the prepared PtRu/C catalysts under 0.5 M H_2SO_4 solution at the scan rate of 20 mV/s: (a) x1, (b) x2, (c) x5, (d) x15, (e) x50 and (f) x250.

charge of the first cycle was 28.5 mC/mg while that of the final cycle was 52 mC/mg. The amount of hydrogen adsorption and desorption generally decrease with the increase of the Ru content in PtRu alloy as hydrogen interacts more with Pt than with Ru. Szabo et al. [28] compared the charges in the hydrogen region using a pure Pt electrode and for a Pt electrode fully covered with Ru. They reported that the amount of hydrogen adsorption on Ru is 15% of that on Pt. Finally, the oxide reduction peak was shifted to a higher potential in PtRu/C. The oxide reduction peak of Pt/C was maintained at 0.76 V in the backward scan while that of PtRu/C changed from 0.43 V to 0.76 V with the cycles. Frelink et al. [29] performed the cyclic voltammetry on a Pt electrode with various amounts of Ru as calculated via the mass change during Ru electrodeposition.

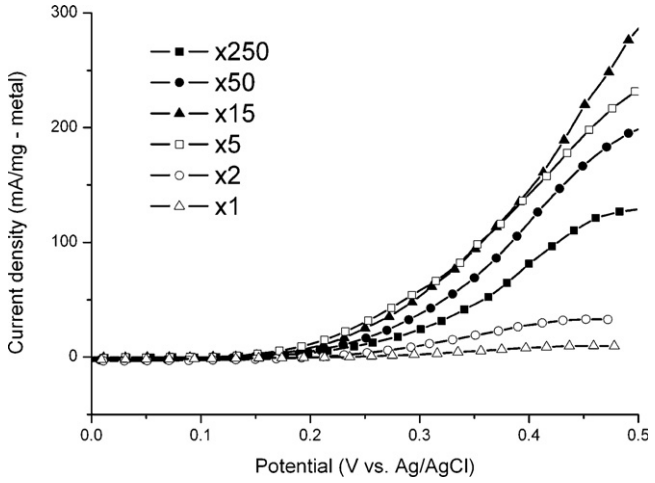

Fig. 6. Linear sweep voltammetry curves of the prepared PtRu/C catalysts under 0.5 M H_2SO_4 + 1 M methanol solution at the scan rate of 1 mV/s.

The oxide reduction peak shifted linearly to the lower potential with the increase of the Ru surface coverage in the PtRu electrode. The decrease of the base current, the increase of the hydrogen desorption charge and the peak shift of the oxide reduction to a higher potential are evidence of the decrease of the Ru surface coverage as the cycles repeat. Furthermore, Ru dissolution into H_2SO_4 solution was confirmed by inductively coupled plasma-mass spectrometer (ICP-MS). Thus, Ru dissolved into the H_2SO_4 solution and the surface composition of Pt increased during the cyclic voltammetry.

Fig. 5 shows cyclic voltammograms of the prepared PtRu/C catalysts. At the initial cycle of the cyclic voltammetry, x1 and x2 showed a large base current, a small hydrogen desorption charge and a low oxide reduction peak compared to other catalysts. From these results x1 and x2 are presumed to have large Ru surface coverage. This Ru-rich surface originated from isolated Ru particles, which could not form a solid solution with Pt. In addition, it was predicted with XRD that x1 and x2 included a small amount of Ru in PtRu solid solution. The cyclic voltammetry patterns of x5, x50 and x250 were similar to that of commercial PtRu/C. On the other hand, the shape of the curve of x15 did not change when compared with other prepared catalysts, implying that x15 formed a stable PtRu solid solution. x15 included a large amount of Ru in the PtRu solid solution in XRD result; therefore, x15 had a stable phase with a high degree of alloying.

Linear sweep voltammetry was performed in order to measure the catalytic activity of methanol electro-oxidation (Fig. 6). All linear sweep voltammetry experiments were accomplished after five cycles of cyclic voltammetry. x5 and x15 showed the highest activities while x1 and x2 showed the lowest. The excess Ru atoms on the catalyst surface of x1 and x2 blocked the active sites of Pt and reduced the activity of metal alloy. Additionally, large crystal size and low dispersion of x1 and x2 reduced the active area of the catalysts.

X-ray photoelectron spectroscopy (XPS) curves of the Pt (4f) region are shown in Fig. 7. Pt, Ru, C and O were found in the XPS results. The surface compositions converted to the ratio of Pt and Ru and the oxidation state of the Pt region are represented in Table 1. The reference binding energies of Pt^0

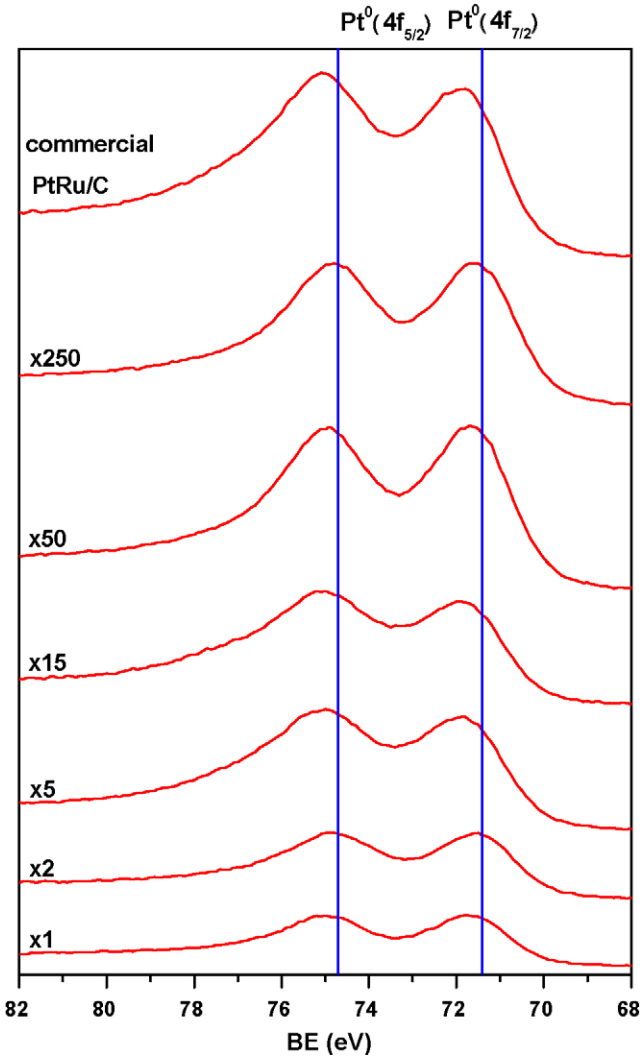

Fig. 7. XPS results of the prepared PtRu/C catalysts in Pt (4f) region.

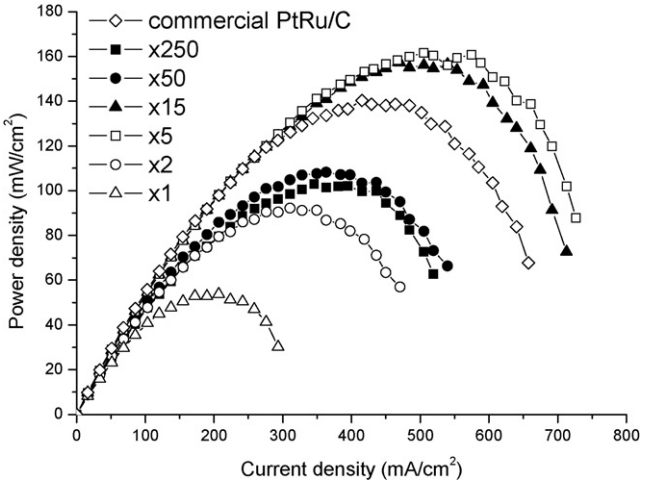

Fig. 8. Unit cell performance using the prepared PtRu/C as anode catalysts (under 60 °C anode: 2 M methanol, cathode: O_2).

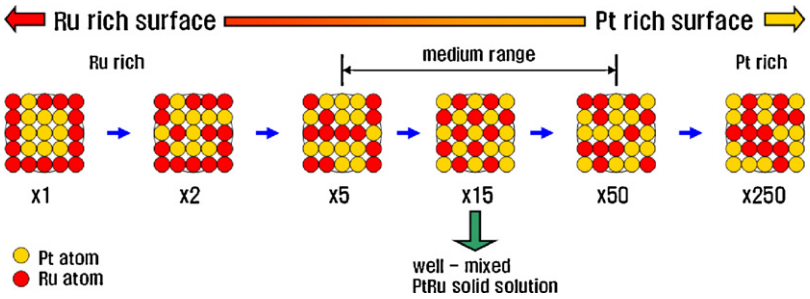

Fig. 9. Surface characteristics of the prepared catalysts in different $NaBH_4$ concentration.

($4f_{5/2}$) and Pt^0 ($4f_{7/2}$) were 74.7 eV and 71.4 eV, respectively [30]. x1 and x2 showed high Ru surface compositions, which coincided with the cyclic voltammetry results. The Ru-rich surface of x1 and x2 was caused by the prior reduction sequence of Pt to Ru in a low reducing agent. For x5, x50 and x250, which were similar to commercial PtRu/C in terms of the cyclic voltammetry, the chemical shift of Pt decreased with the $NaBH_4$ concentration. The increase of the Pt^0 site with the decrease of the Ru composition occurred because the chemical shift of the Pt peaks originated from the interactions between Pt and neighboring Ru. x15 showed the highest oxidation state among the prepared catalysts, which was coincident with the higher peak shift in XRD and the stable cyclic voltammetry pattern. The high methanol oxidation activity of x5 and x15 was mainly caused by the high dispersion of particles and appropriate surface compositions of PtRu.

Unit cell performances for a direct methanol fuel cell were tested using the prepared catalysts as the anode catalyst (Fig. 8). x5 and x15 showed the highest performance among the prepared and the commercial catalysts. The results correlated with the linear sweep voltammetry findings (Fig. 6).

4. Conclusions

PtRu/C catalysts for methanol electro-oxidation were prepared with various $NaBH_4$ concentrations using an impregnation method. The characteristics of the prepared catalyst are as follows:

(1) The catalysts prepared in a low $NaBH_4$ concentration had a Ru-rich surface and large crystals. In addition, they showed aggregated metal particles and low methanol oxidation activity.
(2) In the medium concentration of $NaBH_4$ in which the ratio of $NaBH_4$ to metals was 15, a stable phase PtRu solid solution was created.
(3) The catalysts prepared in the 5 and 15 times $NaBH_4$ concentration of metals showed high methanol oxidation performance, which was due to the high particle dispersion and the appropriate surface composition of PtRu.
(4) In the high $NaBH_4$ concentration, large particles were created and the Pt composition slightly increased.

The prepared catalysts in various $NaHB_4$ concentrations showed not only different surface compositions but also differences in terms of the particle size and level of dispersion. According to the cyclic voltammetry, X-ray photoelectron spectroscopy and X-ray diffraction results, the surface properties of the prepared catalysts can be summarized as shown in Fig. 9. The proper $NaBH_4$ concentration is the medium range in which both the surface composition and the active metal surface area are optimized. Ratio of $NaBH_4$ to metals at 5 and 15 are the optimum point for methanol electro-oxidation according to the findings of this study.

Acknowledgements

This work was supported by the Core technology Development Program for Fuel Cell of Ministry of Commerce, Industry and Energy (MOCIE).

References

[1] H.A. Gasteiger, N. Markovic, P.N. Ross Jr., E.J. Cairns, J. Phys. Chem. 97 (1993) 12020.
[2] J.C. Davies, J. Bonde, A. Logadottir, J.K. Norskov, I. Chorkendorff, Fuel Cells 5 (2005) 429.
[3] D. Chu, S. Gilman, J. Electrochem. Soc. 143 (1996) 1685.
[4] K.T. Jeng, C.C. Chien, N.Y. Hsu, S.C. Yen, S.D. Chiou, S.H. Lin, W.M. Huang, J. Power Sources 160 (2006) 97.
[5] K.I. Han, J.S. Lee, S.O. Park, S.W. Lee, Y.W. Park, H.S. Kim, Electrochem. Acta 50 (2004) 791.
[6] J.S. Guo, G.Q. Sun, Q. Wang, G.X. Wang, Z.H. Zhou, S.H. Tang, L.H. Jiang, B. Zhou, Q. Xin, Carbon 44 (2006) 152.
[7] I.S. Park, K.W. Park, J.H. Choi, C.R. Park, Y.E. Sung, Carbon 45 (2007) 28.
[8] P. Kim, H.S. Kim, J.B. Joo, W.Y. Kim, I.K. Song, J.H. Yi, J. Power Sources 145 (2005) 139.
[9] G.S. Chai, I.S. Shin, J.S. Yu, Adv. Mater. 16 (2004) 2057.
[10] J.H. Choi, K.W. Park, I.S. Park, W.H. Nam, Y.E. Sung, Electrochem. Acta 50 (2004) 787.
[11] J.S. Cooper, P.J. McGinn, J. Power Sources 163 (2006) 330.
[12] A.S. Arico, P.L. Antonucci, E. Modica, V. Baglio, H. Kim, V. Antonucci, Electrochem. Acta 47 (2002) 3723.
[13] A.O. Neto, E.G. Franco, E. Arico, M. Linardi, E.R. Gonzalez, J. Eur. Ceram. Soc. 23 (2003) 2987.
[14] Y.H. Chu, S.W. Ahn, D.Y. Kim, H.J. Kim, Y.G. Shul, H.S. Han, Catal. Today 111 (2006) 176.
[15] W.C. Choi, J.D. Kim, S.I. Woo, Catal. Today 74 (2002) 235.
[16] Z.H. Zhou, W.J. Zhou, S. Wang, G.X. Wang, L.H. Jiang, H.Q. Li, G.Q. Sun, Q. Xin, Catal. Today 93-95 (2004) 523.
[17] M. Watanabe, M. Uchida, S. Motoo, J. Electroanal. Chem. 229 (1987) 395.
[18] K.I. Han, J.S. Lee, H.S. Kim, Electrochem. Acta 52 (2006) 1697.

[19] Y. Shimazaki, Y. Kobayashi, S. Yamada, T. Miwa, M. Konno, J. Colloid Interf. Sci. 292 (2005) 122.
[20] J. Solla-Gullon, F.J. Vidal-Iglesias, V. Montiel, A. Aldaz, Electrochem. Acta 49 (2004) 5079.
[21] D.H. Jung, J.H. Jung, S.H. Hong, D.H. Peck, D.R. Shin, E.S. Kim, Carbon Sci. 4 (2003) 121.
[22] X. Zhang, K.Y. Chan, Chem. Mater. 15 (2003) 451.
[23] Swanson, Tatge, Natl. Bur. Stand. (U.S.), Circ. 539 (1) (1953) 31.
[24] S.A. Lee, K.W. Park, J.H. Choi, B.K. Kwon, Y.E. Sung, J. Electrochem. Soc. 149 (2002) A1299.
[25] T.W. Kim, S.J. Park, L.E. Jones, M.F. Toney, K.W. Park, Y.E. Sung, J. Phys. Chem. B 109 (2005) 12845.
[26] S.Lj. Gojkovic, T.R. Vidakovic, D.R. Durovic, Electrochem. Acta 48 (2003) 3607.
[27] R.O. Lezna, N.R. De Tacconi, A.J. Arvia, J. Electroanal. Chem. 151 (1983) 193.
[28] S. Szabo, I. Bakos, F. Nagy, J. Electroanal. Chem. 271 (1989) 269.
[29] T. Frelink, W. Visscher, J.A.R. van Veen, Langmuir 12 (1996) 3702.
[30] R.K. Raman, A.K. Shukla, A. Gayen, M.S. Hegde, K.R. Priolkar, P.R. Sarode, S. Emura, J. Power Sources 157 (2006) 45.